1. Reuse of PVC Waste and Its Transformation into Functional Electrospun Membrane to Remove Organic Dyes from Aqueous Solutions

Katarzyna Prus[1], Aleeza Khurram[2], Emilia Karpiel[2], Paulina Pietrzyk-Thel[1], Sławomir Wilczewski[3*], Marianna Gniadek[4], Adrianna Nowak[1], Agata Roszkiewicz[1], Njemuwa Nwaji[1], Justyna Widera-Kalinowska[2], Michael Giersig[1], Magdalena Osial[1*]

[1] Institute of Fundamental Technological Research, Polish Academy of Sciences
Warsaw, Poland
[2] Department of Chemistry, Adelphi University
Garden City, NY, USA
[3] Faculty of Chemical Technology and Engineering,
Bydgoszcz University of Science and Technology
Bydgoszcz, Poland
[4] Faculty of Chemistry, University of Warsaw
Warsaw, Poland
[*] Corresponding Authors: slawomir.wilczewski@pbs.edu.pl, mosial@ippt.pan.pl

The membrane technology in water treatment and desalination offers great potential in thin-film composite nanofiltration. This study utilized the electrospinning approach to fabricate nanofibers from recycled plasticized and unplasticized poly(vinyl chloride) (PVC) as a membrane for effective wastewater purification. The physicochemical properties and purification performance of the membranes were investigated. The obtained membrane showed potential as an adsorbent for cationic dyes in water. The pH-dependent study revealed optimal activity at pH of 7.0 for crystal violet (CV) and pH of 10 for methyl violet (MV) with plasticized PVC (PVC-P) showing enhanced ability compared to unplasticized PVC (PVC-R). Additionally, PVC-P shows a dye removal efficiency of 80 % and 55 % for CV and MV, respectively. Thus, the study could serve as an innovative dual-purpose approach to recycling spent PVC-based materials and wastewater treatment. The thermogravimetric analysis and tensile tests revealed that PVC-R fibers exhibited higher thermal stability ($T_{\mathrm{onset}} \approx 282\,^{\circ}\mathrm{C}$) and tensile strength (∼10.6 MPa) com-

pared to PVC-P fibers, while PVC-P fibers showed greater elasticity (elongation at break ∼40 %) but lower thermal resistance ($T_{\text{onset}} \approx 250\,^{\circ}\text{C}$). These results highlight the distinct structural behavior of rigid and plasticized PVC fibers under thermal and mechanical stress.
Keywords: PVC waste, adsorption, recycling, crystal violet, methyl violet, electrospun fibers.

https://doi.org/10.24423/9788365550682.ch1

Symbols and abbreviations

20/100/PVC-P – membrane based on PVC-P obtained at conditions: 20 kV and 100 µL min^{-1},
20/150/PVC-P – membrane based on PVC-P obtained at conditions: 20 kV and 150 µL min^{-1},
23/100/PVC-P – membrane based on PVC-P obtained at conditions: 23 kV and 100 µL min^{-1},
23/150/PVC-P – membrane based on PVC-P obtained at conditions: 23 kV and 150 µL min^{-1},
20/100/PVC-R – membrane based on PVC-R obtained at conditions: 20 kV and 100 µL min^{-1},
20/150/PVC-R – membrane based on PVC-R obtained at conditions: 20 kV and 150 µL min^{-1},
23/100/PVC-R – membrane based on PVC-R obtained at conditions: 23 kV and 100 µL min^{-1},
23/150/PVC-R – membrane based on PVC-R obtained at conditions: 23 kV and 150 µL min^{-1},
C_0 – initial concentration of dye solution [$\text{mol} \cdot \text{dm}^{-3}$],
C_x – concentration of the dye after adsorption [$\text{mol} \cdot \text{dm}^{-3}$],
CV – crystal violet,
DINP – diisononyl phthalate,
DMF – dimethylformamide,
$H\%$ – adsorption effectiveness,
k – adsorption rate constant,
k_1 – adsorption rate constants for the pseudo-first-order kinetic model,
k_2 – adsorption rate constants for the pseudo-second-order kinetic model,
KNO_3 – potassium nitrate,
m – mass of adsorbent [g],
MV – methyl violet,
NaCl – sodium chloride,
NaOH – sodium hydroxide,
pH_{ZPC} – pH at zero point of charge,
PVC-R – unplasticized PVC,
PVC-P – plasticized PVC,
R^2 – correlation coefficient,
SEM – scanning electron microscopy,
THF – tetrahydrofuran,

t – time [s],
TGA – thermogravimetry,
T_{onset} – onset temperature,
Q_e – amount of adsorbate at equilibrium,
Q_t – amount of adsorbate at a time t,
UV-vis – ultraviolet-visible light,
V – volume [dm^{-3}].

1. Introduction

Poly(vinyl chloride) (PVC) is an extensively utilized thermoplastic polymer widely used in daily life for its performance, including chemical and weathering resistance. Additionally, its broad use leads to the generation of post-consumer and post-process waste. This waste can be reprocessed; however, conventional mechanical and thermal recycling routes face important constraints arising from the diversity of formulation additives that affect processing and define end-use properties. Repeated reprocessing is further hindered by the inherently low thermal stability of PVC leading to partial or even extensive degradation, requiring moderation of the processing conditions. These limitations motivate the development of innovative methods for PVC reuse. Solvent-based dissolution emerges as a promising complementary route, as it enables the removal of low-molecular-weight additives from polymer blends and/or targeted re-modification of their properties [1–4].

The service performance of PVC strongly depends on the presence of plasticizers and other modifiers. Unplasticized PVC (PVC-R) is a rigid, durable, chemically resistant and UV-resistant polymer, widely used in building products such as window frames, water pipes, fencing, and other industrial applications. Plasticized PVC (PVC-P) incorporates low-molecular-weight plasticizers that reduce interchain interactions, improving flexibility and low-temperature performance. PVC-P is typically used in cable insulations, automotive interiors, floor coverings, and coating layers [1, 5]. Depending on additives such as plasticizers the recycling of PVC remains challenging and requires a change of experimental conditions during processing. Dissolution of PVC as a complementary recycling technique allows the use of other techniques, including electrospinning which enables fibrous structures fabrication. However, in the case of PVC, the process is limited by the low solubility of the polymer in typical organic solvents and the relatively high viscosity of its solutions. Previous studies on the electrospinning of poly(vinyl chloride) were concerned with the pristine polymer and focused primarily on the selection of solvent and their mixtures (mainly DMF and THF) [6], as well as on the optimization of electrospinning parameters such as the polymer concentration, applied voltage, and flow rate of the solution in order to obtain

uniform nanofibers with the desired diameter [7, 8]. Electrospinning also enables incorporation of other ingredients such as plasticizers or other organic materials, e.g. PVP and/or inorganic fillers, e.g. MWCNTs [9], silver and titanium dioxide [10] to modify physicochemical characteristics of the material, including adsorptive properties.

The obtained PVC fibers were characterized by a large specific surface area, flexibility, and good dielectric properties, which create prospects for their application in insulations and filtration technologies [11, 12].

In this work, we present results on the use of electrospinning in the recycling of plasticized and unplasticized PVC waste to fabricate fibrous membranes to be used in water purification. Membranes were used to remove cationic dyes such as crystal violet and methyl violet 2B which are emerging contaminants affecting ecosystems [13–15] from aqueous solutions. Besides that, thermal and mechanical properties were examined. Unlike previously reported studies focused mainly on the electrospinning of pristine or modified PVC with synthetic fillers, the present research introduces a novel approach that utilizes both aged unplasticized (PVC-R) and plasticized (PVC-P) post-consumer wastes as precursors for electrospun nanofibrous membranes. This dual-purpose strategy simultaneously addresses the challenges of PVC recycling and the development of efficient, low-cost adsorptive materials for wastewater treatment, which has not been previously reported in the literature.

2. Experimental

2.1. Chemicals and methods

Poly(vinyl chloride) nanofibers were produced from a blend of unplasticized PVC S61 (Anwil S.A., Włocławek, Poland) with the following composition: Poly(vinyl chloride) PVC Neralit 601 100 phr, Organotin Patstab 2310 2 phr, Calcium stearate Ceasit I 1.2 phr, Fatty acid ester Loxiol G-32 1.5 phr, Acrylic-based polymer Poraloid K-125 1 phr, Acrylic-based polymer Poraloid K-175 1 phr, Paraffin Naftolube FTP 0.5 phr. Diisononyl phthalate (Sigma-Aldrich) was used as a plasticizer. Tetrahydrofuran (Sigma-Aldrich) and Dimethylformamide (Sigma-Aldrich) were used to prepare PVC solutions. Crystal violet, methyl violet, KNO_3, and NaOH were supplied by Warchem Sp. z o.o., Warsaw, Poland. HCl was supplied from POCH, Gliwice, Poland. Water was purified using HYDROLAB water filtering system, HYDROLAB, Gliwice, Poland.

Tensile properties were determined on strips 50 mm in length, 10 mm in width, and 0.06 $\pm$0.005 mm in thickness (gauge length 30 mm). Measurements were performed on a Zwick/Roell Z010 testing machine (Ulm, Germany) at 23 °C, with a crosshead speed of 10 mm/min. Thermogravimetric analysis (TGA) was performed using a TG 209 F3 device (Netzsch Group, Germany) in the temperature

range from 30 °C to 600 °C at a heating rate of 10 °C/min under a nitrogen atmosphere. The morphology of electrospun PVC-based materials was studied using Scanning Electron Microscopy (SEM), Merlin, Carl Zeiss, Stuttgart, Germany. The contact angle was measured using the Ossila L2004 goniometer by placing 1 µL of distilled water onto the PVC-P and PVC-R materials. The measurement was performed 20 times, with each droplet placed in a different location on the material. The pH was measured with the Elmetron CP-411 pH-meter. The UV-vis spectrometer Lambda1050+ (PerkinElmer) was used to measure the adsorption effectiveness. Determination of the functional groups in the materials was performed using the SpectrumTwo ATR (Perkin Elmer), while the Thermogravimetric Analyzer (TGA) TG8000 (Perkin Elmer) was used to determine the thermal stability of the materials. UV-vis, ATR, and TGA were supplied by the Pro-Environment Sp. z o.o., Warsaw, Poland.

2.2. Procedures

2.2.1. Preparation and aging of poly(vinyl chloride)

Unplasticized poly(vinyl chloride), also called rigid PVC (PVC-R), samples were prepared by extrusion and pressing. PVC was extruded using the co-rotating twin-screw extruder EHP-2x24 M (Zamak Mercator Ltd.) at a maximum temperature of 185 °C. Then, the material was granulated and pressed using a hydraulic press. The pressing process parameters were: temperature 190 °C, pressure 100 bar, time 5 min. Plates with dimensions of $120 \times 120 \times 2$ mm were obtained. Plasticized PVC (PVC-P) plates were prepared by mixing the PVC dry blend with a diisononyl phthalate (DINP), which is a widely used plasticizer in PVC materials production (50 phr) at 110 °C for 2 h. The prepared blend was extruded and pressed in the same way as unplasticized PVC, but the maximum extrusion temperature was 165 °C, and the pressing temperature was 170 °C. The obtained materials were subjected to photodegradation and thermal aging (exposure to UV radiation and high temperature of 70 °C for 500 h).

2.2.2. Methodology of electrospinning of PVC

To produce electrospun PVC nanofibers, the polymer plates obtained after accelerated degradation were ground and dissolved in a THF/DMF mixture (1:1 w/w), producing 20 % PVC-R and PVC-P solutions, respectively. Electrospinning was carried out on a custom-built apparatus under the following parameters: voltages of 20 kV and 23 kV, flow rates of 100 µL min^{-1} and 150 µL min^{-1}, the needle-to-collector distance of 10 cm. Electrospinning was performed on a fixed metal plate covered with aluminum foil, using 5 mL of solution for each sample. The materials were labeled as follows: for nanofibers obtained at 20 kV and 150 µL min^{-1} from unplasticized PVC, the sample designation was 20/150/PVC-R. Similarly, samples obtained under 23 kV and 150 µL min^{-1}, 20 kV and

100 µL min^{-1}, 23 kV and 100 µL min^{-1} were labeled as 23/150/PVC-R, 20/100/PVC-R, 23/100/PVC-R, respectively. PVC-P samples were labeled in the same way, using PVC-P abbreviation: 20/150/PVC-P, 23/150/PVC-P, 20/100/PVC-P, and 23/100/PVC-P.

3. Results

3.1. Selection of electrospinning parameters for aged rigid and soft PVC

The selection of appropriate electrospinning parameters for plasticized and rigid PVC was based on thermal analysis and mechanical properties of the obtained fibrous mats. Table 1 shows thermal stability, tensile strength, and elongation at break for fibers obtained under all tested electrospinning conditions. As can be seen, depending on the experimental conditions during the electrospinning, samples are characterized by different mechanical properties. The highest thermal stability, tensile strength, and resistance to stretching among PVC-R and PVC-P samples show 23/150/PVC-R and 20/100/PVC-P samples.

Table 1. Thermal stability and mechanical properties of PVC-R and PVC-P fibers obtained under different electrospinning conditions.

Electrospinning parameter	T_{onset} [°C]	Tensile strength [MPa]	Elongation at tensile strength [%]
20/100/PVC-R	277.7 ±0.5	10.5 ±1.8	1.4 ±0.1
20/150/PVC-R	279.9 ±0.3	6.3 ±1.9	1.1 ±0.3
23/100/PVC-R	270.6 ±0.7	6.8 ±1.7	1.4 ±1.2
23/150/PVC-R	282.0 ±0.2	10.6 ±1.8	1.8 ±0.3
20/100/PVC-P	249.7 ±0.9	4.0 ±0.8	39.6 ±6.4
20/150/PVC-P	236.4 ±1.0	1.9 ±0.5	34.7 ±3.7
23/100/PVC-P	235.8 ±2.1	2.5 ±0.1	34.8 ±3.0
23/150/PVC-P	228.5 ±3.4	2.7 ±1.1	40.4 ±5.8

Figures 1a and 1b present the TGA curves and tensile curves, respectively, for materials obtained under the most favorable electrospinning conditions. Thermal analysis revealed that PVC fiber degradation followed the typical two-stage pattern for this polymer. The first stage, associated with polymer dehydrochlorination, occurred between ∼150 °C and 325 °C. The second stage, between 350 °C and 425 °C, corresponds to carbon-based chain degradation. PVC-R exhibits higher thermal stability than PVC-P, which relates to the presence of plasticizer that changes durability and mechanical properties of the material [16–19]. In PVC-R, an additional degradation stage was observed up to ∼125 °C, which

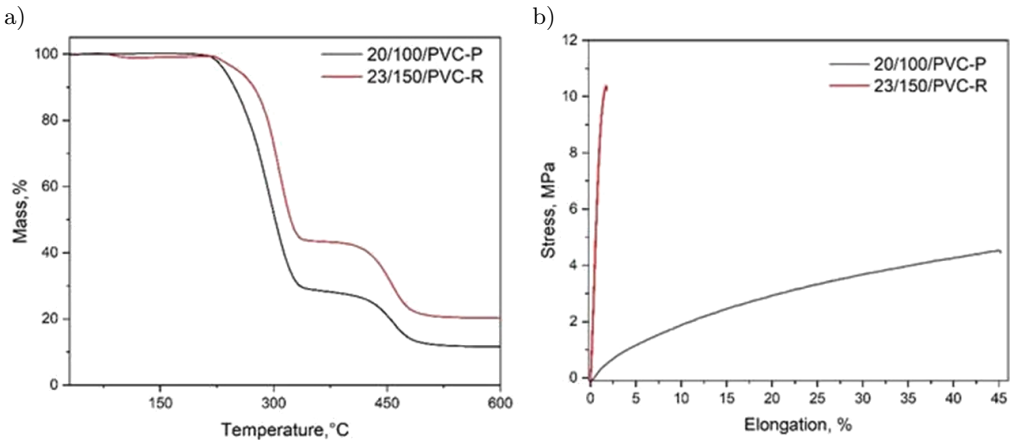

Fig. 1. a) TGA curves, and b) stress change as a function of elongation of PVC-R and PVC-P fiber-based membranes.

is assigned to solvent residue evaporation. This stage was absent in PVC-P, suggesting strong binding of the plasticizer to the polymer [20, 21]. Due to solvent residues, found mainly in PVC-R samples, the extrapolated onset temperature (T_{onset}) was used as a measure of thermal stability. Based on the analysis, the most favorable electrospinning conditions for aged PVC-R were 23 kV and 150 µL min^{-1}, and for PVC-P, 20 kV and 100 µL min^{-1}.

Figure 1b shows the tensile curves, and the tensile strength and elongation at break for electrospun mats from PVC-P and PVC-R, which are presented in Table 1. PVC-R samples showed significantly higher tensile strength, reaching 10.6 MPa for 23/150/PVC-R, but low elongation at break (∼2 %), which is indicative of high stiffness and brittleness for this material. The sharp increase in stress at low strain suggests limited ability of PVC-R fibers to reorganize and undergo plastic deformation before failure. PVC-P samples displayed the opposite trend, reaching the maximum tensile strength of 4.0 MPa (20/100/PVC-P) and elongation at break of ∼40 % [22, 23]. The gradual increase in stress with strain and the absence of a clear yield point are characteristic of materials with high flexibility and chain mobility. The results confirm that the presence of plasticizer significantly modifies the mechanical properties of PVC-based electrospun mats, increasing deformability of the material. The applied plasticizer was strongly bound to the polymer chain and did not migrate into the solvents, as evidenced by the mechanical properties typical of plasticized PVC [20, 24].

These results indicate that the selection of electrospinning parameters for aged PVC fibers should be matched to the polymer type and application requirements. For the tested PVC blends, the most favorable parameters were 23 kV and 150 µL min^{-1} for PVC-R, and 20 kV and 100 µL min^{-1} for PVC-P. Further studies were carried out using materials produced under these conditions.

3.2. Morphology and contact angle measurements

Morphology studies using the Scanning Electron Microscopy (SEM) clearly show differences between the PVC-P and PVC-R, indicating a key role of the plasticizer in the electrospinning of the fibrous membrane. In Fig. 2a PVC-P-based material reveals a textile-like structure made of micron-sized fibers that stack to each other forming flat, tight and highly porous membranes. The lack of plasticizer in the PVC-R sample caused a much looser structure made of much thicker fibers compared to the PVC-P. The images presented in Fig. 2b illustrate distilled water droplets onto PVC-P and PVC-R samples, where differences in the contact angle are seen. The contact angle for PVC-R is about 94.36 ±2.58, PVC-P is about 84.81 ±3.99. These values are much lower than the contact angle presented in the literature for the PVC-based electrospun fibers [25], which can be caused by different fibers morphology. Lower values result in more effective wetting of the membrane that can work not only as the mechanical barrier for the particle-based water pollutants but also as the adsorbent.

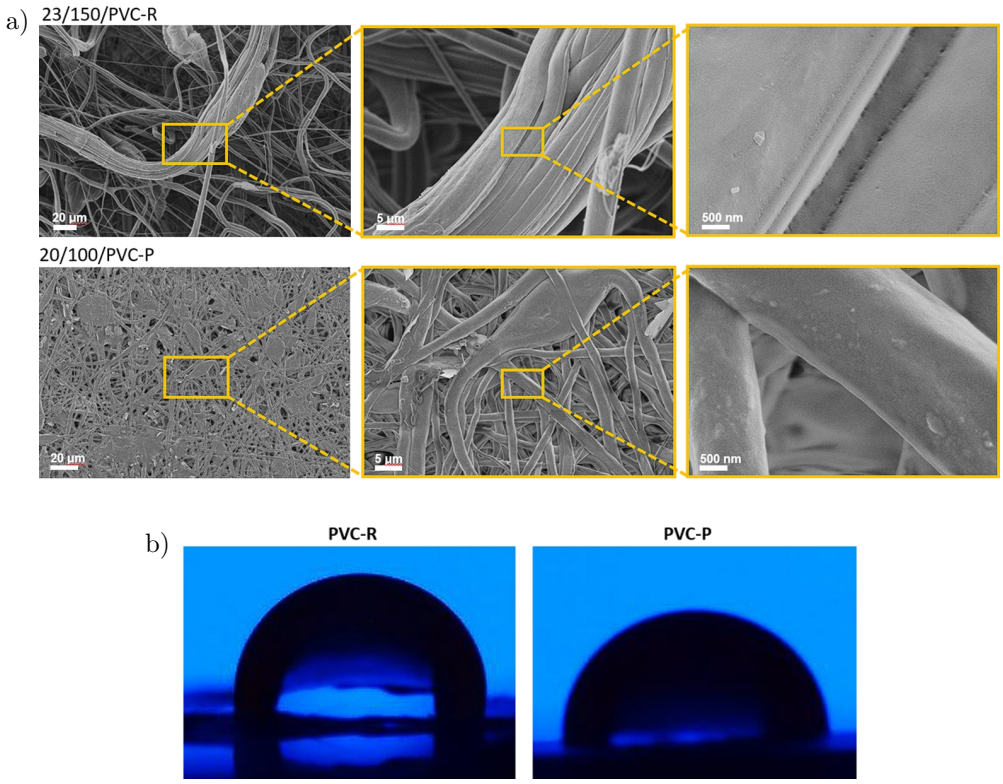

Fig. 2. a) SEM images, and b) images from the contact angle measurement for 23/150/PVC-R and 20/100/PVC-P.

3.3. Adsorption studies

The proposed electrospun membranes based on the recycled PVC were tested as adsorbents on dye-based organic pollutants. First, the point of zero charge (pH_{ZPC}) was measured to determine the affinity of the proposed membranes to cationic or anionic dyes. Measurements were performed in 0.05 M KNO_3, where 30 mg of both materials, PVC-R and PVC-P, were added to the 30 mL of solution, and the pH change after 24 h was recorded; pH was set using HCl and NaOH. As can be seen in Fig. 3a, the isoelectric point is about 5.92 for PVC-R and 5.82 for

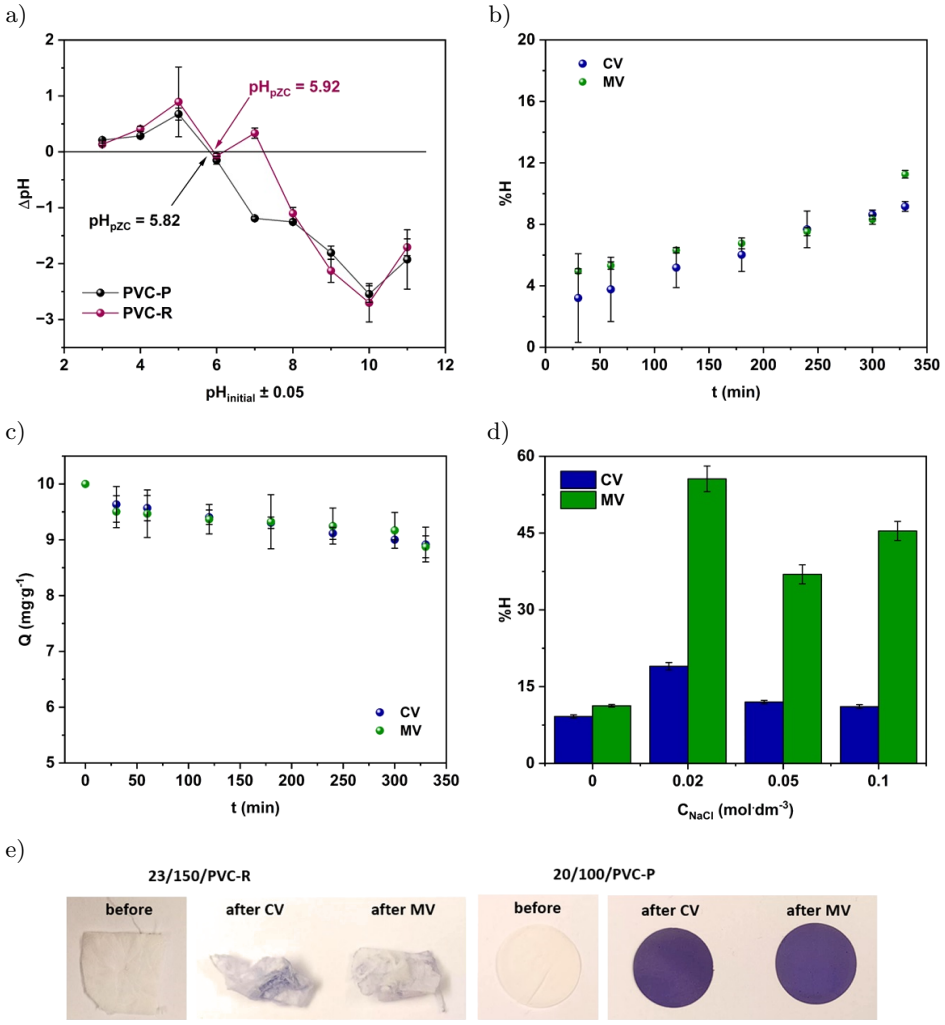

Fig. 3. a) pHPZC study for both materials (20/100/PVC-R and 23/150/PVC-P), adsorption effectiveness of CV and MV 20/100/PVC-R: b) as a function of time at pH 8.0, c) change of the dye concentration as a function of time, d) in different ionic strength moderated with NaCl.

PVC-P, while positive charge occurs below pH_{ZPC} and negative charge appears in the alkali media. The obtained values are similar to the pH_{ZPC} presented in the literature for PVC-based microplastics that may contain different additives, e.g., 5.8 [26], 6.43 [27]. A similar trend is recorded for both PVC-R and PVC-P-based materials. Therefore, cationic dyes, in particular crystal violet (CV) and methyl violet 2B (MV), were chosen as model pollutants in adsorption studies for the negative charge appearance onto membranes in the alkali media. As can be seen, the PVC-P may adsorb cationic dyes even in the neutral pH, while for PVC-R the surface may have a positive charge, which can affect cationic dyes removal in neutral pH.

The adsorption studies were performed using 10 ppm of both CV and MV dyes, where 30 mg of adsorbents, 23/150/PVC-R and 20/100/PVC-P, were added to 30 mL of CV and MV solutions. Then, the solution was mixed using a magnetic stirrer (250 rpm) for the uniform wetting of the fibrous membrane in the solution. Importantly, PVC-P samples tend to wet more effectively than PVC-R ones but undergo disassembly under mixing into separate fibers that can relate to the lower contact angle after the plasticizer introduction into the PVC-R. The adsorption effectiveness ($H\%$) was estimated using Eq. (1) [28]:

$$H\% = \frac{C_0 - C_x}{C_0} \times 100\,\%, \tag{1}$$

where C_0 is an initial concentration of dye solution [$\mathrm{mol \cdot dm^{-3}}$]; C_x stands for the concentration of the dye after adsorption [$\mathrm{mol \cdot dm^{-3}}$].

The adsorption effectiveness reaches just ∼8 % for CV removal and similarly ∼10 % for MV as seen in Fig. 3b. Moreover the change of dye concentration during the adsorption process also was not effective (Fig. 3c). However, with increasing ionic strength the effectiveness of adsorption processes was improving: for concentration of 0.02 $\mathrm{mol \cdot dm^{-3}}$ the $H\%$ removal of MV is about 60 %, while for CV about 15 %. Therefore, increasing NaCl concentration in the solution causes a decrease in the effectiveness of the adsorption process to ∼45 % for MV and ∼10 % for CV, respectively. Importantly, the PVC-R-based membrane changes its texture in the solution into fibrous, making it difficult to remove from the aqueous solutions. Figure 3e shows both 20/100/PVC-P and 23/150/PVC-R samples before and after the CV and MV treatment, where the removal effectiveness is clearly seen through the different coloration with dyes. The increase in ionic strength even worsened the texture, so for the following adsorption effectiveness studies at various pH the 20/100/PVC-P sample was chosen.

The adsorption capacity during the time (Q_t) was estimated using Eq. (2) [28] as follows:

$$Q_t = \frac{(C_0 - C_x) \times V}{m}, \tag{2}$$

where C_0 – initial concentration of dye solution [mol · dm^{-3}], C_x – concentration of the dye after adsorption [mol · dm^{-3}], V – volume [dm^{-3}], m – mass of adsorbent [g].

Complementary to the spectrophotometric analysis, both types of membranes were investigated with FTIR before and after the adsorption of CV and MV to confirm the effectiveness of adsorption. First, bare 23/150/PVC-R and 20/100/PVC-P materials were compared to ascribe the peaks that are related to the presence of plasticizer in the material. Figure 4a shows normalized T% spectra, where the peaks located around (608, 637, 699, and 741) cm^{-1} can be ascribed to the C–Cl vibration in the PVC chain and/or peaks at 699 cm^{-1} and 741 cm^{-1} can come from the out-of-plane and in-plane aromatic ring bending, respectively. The following peak at 951 cm^{-1} relates to ν(C–H) vibration in CH_2 of the alkyl chain. The peak 1041 cm^{-1} that appears in PVC-P comes from the C–O vibrations from the DINP plasticizer. For the PVC-R sample, a minor peak located at 1069 cm^{-1} is recorded. Its presence can be related to the C–O vibration from the solvent residues in the polymer matrix. A sharp peak that appears at 1123 cm^{-1} in the PVC-P sample can be ascribed to the C–O–C vibration from the DINP plasticizer, while the peaks at 1202 cm^{-1} possibly come from C–C and/or C–O vibrations. The following peaks at 1256 cm^{-1} and 1273 cm^{-1} can be related to the C–O stretching and C–N stretching, respectively. Next, 1424 cm^{-1} and 1461 cm^{-1} can also be related to the –C–H bending vibrations, while the peaks located at 1578 cm^{-1} and 1593 cm^{-1} that are seen in the PVC-P sample are characteristic of the C=C stretching in the aromatic ring from the DINP plasticizer, likewise, the peak at 1720 cm^{-1} comes from C=O vibration in DINP. Bands located at 2849 cm^{-1} and 2917 cm^{-1} are characteristic of the symmetric and asymmetric vibrations of CH_2 group, while bands at 2870 cm^{-1} and 2956 cm^{-1} can be ascribed to symmetric and asymmetric vibrations in CH_3

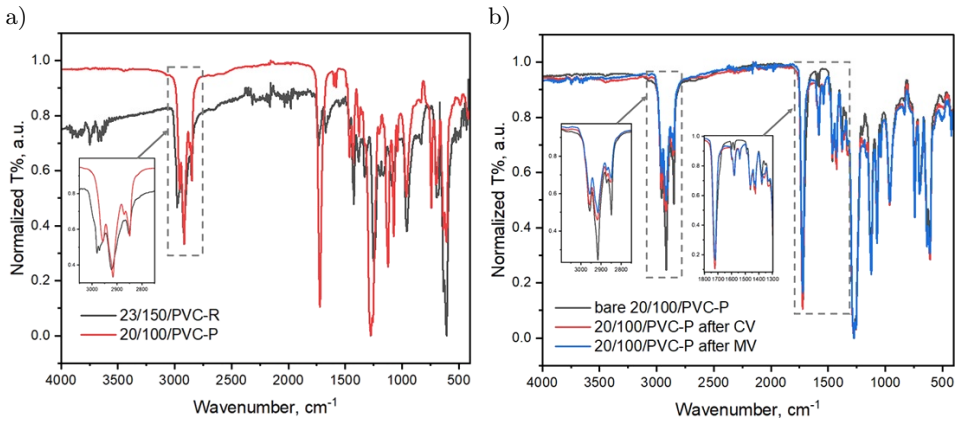

Fig. 4. Normalized FTIR spectra of a) bare 23/150/PVC-R and 20/100/PVC-P, and b) 20/100/PVC-P before and after CV and MV treatment.

functional groups in the alkyl chain [29]. The different intensities, as well as the number of bands, come from the compositional differences related to the plasticizer presence in the PVP-P sample. The spectra of PVC-P before and after CV and MV treatment, that are presented in Fig. 4b, confirm the dyes' adsorption onto the adsorbent through the appearance of a band located at 1539 cm^{-1} that relates to the N–H vibration in the dye molecules adsorbed onto the membranes, as well as through the different ratio between $–CH_2$ and $–CH_3$-related bands in the 2800–3000 cm^{-1} region. Additionally, the shift of the band at 1202 cm^{-1} toward lower wavenumbers and a shift of the bands at 1164 cm^{-1} are in the region for C–O–C and/or C–N vibrations. The changes in the spectra after dyes' adsorption come from the intermolecular interactions between the membrane and dyes through the electrostatic interactions, hydrogen bonds, van der Waals, and/or π–π interactions (rings in the dye and plasticizer).

As the wastewater can have a different pH, its influence on the $H\%$ was evaluated, where the contact time of about 550 min was chosen. Adsorption studies performed in solutions of different pH show that 20/100/PVC-P is an effective adsorbent. Due to this, the effectiveness increased to ∼80 % for CV, and to ∼55 % for MV, at the same pH value, respectively (Fig. 5a). The amount of remain-

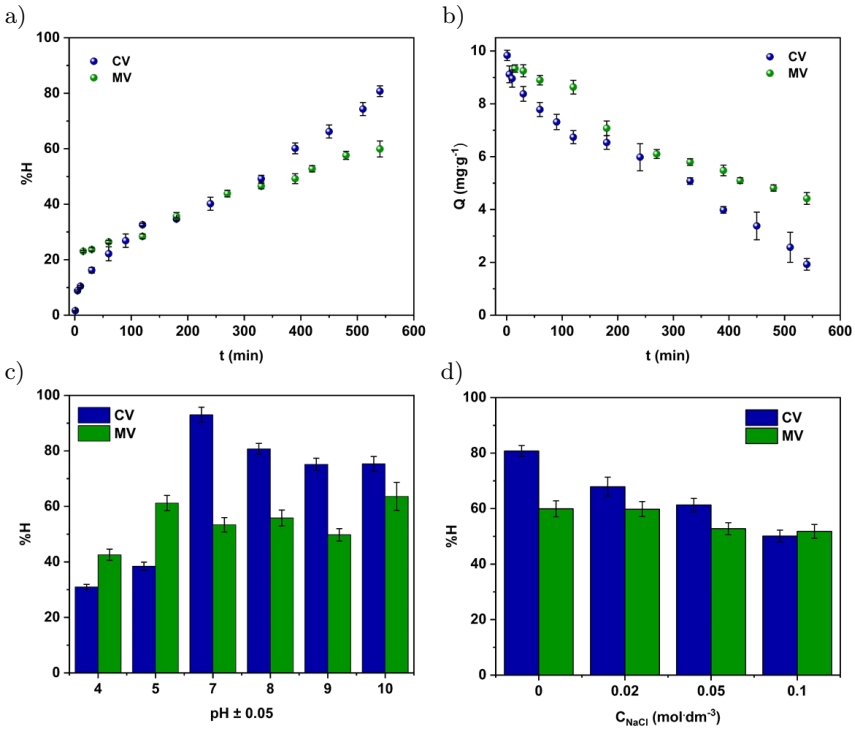

Fig. 5. Adsorption effectiveness of CV and MV of 20/100/PVC-P: a) as a function of time at pH 8.0, b) change the dye concentration as a function of time, c) in various pH ranges, d) in relationship to the varying ionic strength.

ing dyes after the process was $\sim 1.5\,\mathrm{mg \cdot g^{-1}}$ for CV, and $4.3\,\mathrm{mg \cdot g^{-1}}$ for MV (Fig. 5b). However, the highest effectiveness was recorded for pH 7.0 for CV and 10.0 for MV. It is associated with the negative charge of the membrane at those pH values (Fig. 5). Nevertheless, with the increasing salinity of the solutions, the effectiveness of the adsorption process decreases of about $\sim 5\,\%$ for MV, and 30 % for CV, respectively (Fig. 5d). For comparison, commercial polymeric membranes such as PVDF, PAN, or PES typically achieve cationic dye removal efficiencies of 60 % to 90 % depending on surface modification [30–34]. The adsorption performance of the PVC-P membrane (80 % for CV and 55 % for MV) is therefore comparable to or only slightly lower than that of modified commercial membranes, confirming its potential as a cost-effective and sustainable alternative derived from recycled waste.

The kinetic study of 20/100/PVC-P material was investigated at pH equal to 8.0 and 7.0, where the highest CV and MV removal effectiveness was measured, using linear equations (3) and (4) for:

– pseudo-first-linear order:

$$\log\left(Q_e - Q_t\right) = \log Q_e - \left(\frac{k_1}{2.303}\right) t, \tag{3}$$

– pseudo-second-linear order:

$$\frac{t}{Q_t} = \frac{1}{k_2} Q_e^2 + \frac{t}{Q_e}, \tag{4}$$

where Q_e – amount of adsorbate at equilibrium; Q_t – amount of adsorbate at time t; k_1 and k_2 – adsorption rate constants for the pseudo-first-order and pseudo-second-order kinetic models, respectively.

Based on the correlation coefficient (R^2) the adsorption process for the data presented in Fig. 6 for both dyes in both pH conditions undergoes pseudo-first-order kinetics. Importantly, as the amount of adsorbent from the calculations corresponds to the amount of adsorbent from the experimental data, it means that both substances achieved an equilibrium state. Table 2 shows a set of parameters for different kinetic models.

The adsorption of CV and MV onto 20/100/PVC-P is based on the physical interactions, where adsorption is faster at the initial stage for the access to many active sites on the surface of the membrane. Then, it slows down as active sites get filled with adsorbed molecules as long as the adsorbent reaches equilibrium, where the active sites are no longer available. As the studies confirm only weak interactions between the membrane and dye-based model pollutants, the adsorbent can be reused; however, the desorption of the dyes should be optimized.

Membranes made of bare PVC are not commonly reported in the literature for the removal of different types of organic dyes. Literature shows mainly

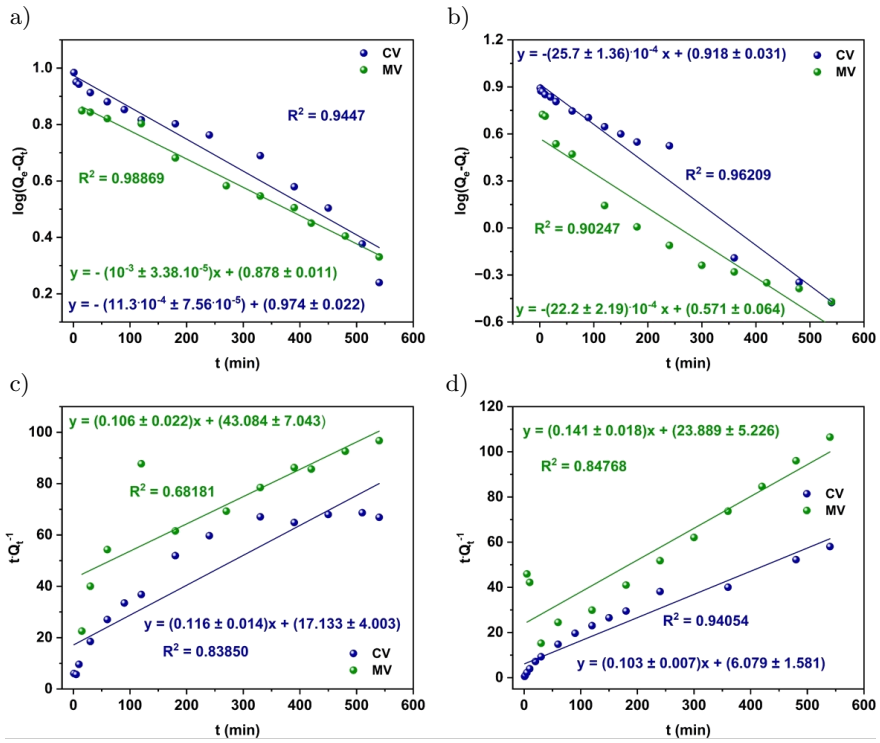

Fig. 6. Linear kinetics order at various pH values for 23/150/PVC-P sample: a) I kinetic order at pH equal 8.0, b) I kinetic order at pH equal 7.0, c) II kinetic order at pH equal 8.0, d) II kinetic order at pH equal 7.0.

Table 2. Parameters of fitting kinetics order for PVC-P at different pH values.

Dye	pH range	Kinetic order	Q_{exp} $[\text{mg}\cdot\text{g}^{-1}]$	Q_{cal} $[\text{mg}\cdot\text{g}^{-1}]$	k	R^2
CV	pH 8.0	pseudo-first	9.812 ±0.343	9.419 ±0.174	$2.602\cdot10^{-3}$ $\pm1.742\cdot10^{-4}$ min^{-1}	0.9447
MV			7.724 ±0.309	7.554 ±0.078	$2.303\cdot10^{-3}$ $\pm7.803\cdot10^{-5}$ min^{-1}	0.98869
CV		pseudo-second	9.812 ±0.343	8.584 ±0.071	4.301 ±0.184 $\text{g}\cdot\text{mg}^{-1}\cdot\text{min}^{-1}$	0.83850
MV			7.724 ±0.309	9.412 ±0.045	2.057 ±0.126 $\text{g}\cdot\text{mg}^{-1}\cdot\text{min}^{-1}$	0.68181
CV	pH 7.0	pseudo-first	9.637 ±0.385	8.276 ±0.031	$5.919\cdot10^{-3}$ $\pm3.137\cdot10^{-4}$ min^{-1}	0.98869
MV			5.409 ±0.135	3.724 ±0.504	$5.113\cdot10^{-3}$ $\pm5.042\cdot10^{-4}$ min^{-1}	0.90247
CV		pseudo-second	9.637 ±0.385	9.741 ±0.145	8.287 ±0.057 $\text{g}\cdot\text{mg}^{-1}\cdot\text{min}^{-1}$	0.94054
MV			5.409 ±0.135	7.097 ±0.056	3.972 ±0.009 $\text{g}\cdot\text{mg}^{-1}\cdot\text{min}^{-1}$	0.84768

PVC-based composites to be used for membrane fabrication. Agaguena *et al.* [35] reported the adsorption of methylene blue by a membrane composed of PVC/ PVC-based copolymer with PDMAEM(N+) reaching 87.23 % adsorption efficiency of methylene blue. However, for crystal violet, the H% was only about

1.66 % at pH 7.0, and the process followed a pseudo-second-order kinetic model [35]. Landarani *et al.* [36] presented an iron(III)–polyvinyl chloride (PVC)–Schiff base adsorbent for the removal of methyl orange, achieving nearly 90 % removal at a dye concentration of 20 ppm at pH 7.0, following a pseudo-second-order kinetic model. The $H\%$ values presented in this work are much higher than those that are mentioned in the literature for differing materials. The effect relates to the different composition and morphology of the membranes resulting in different interactions between the dyes and a surface of the membrane.

4. Conclusions

Recycling of poly(vinyl chloride) is hindered due to low thermal stability of the polymer as well as the use of various organic and mineral additives during its processing. In this work, we present a simple method for reusing PVC waste, based on its dissolution in an organic solvent followed by electrospinning, to prepare a textile-like membrane made of fibers for water purification. To obtain the membrane with desired physicochemical characteristics, unplasticized PVC and PVC containing DINP plasticizer were used. The SEM images revealed differences in the plasticized and unplasticized electrospun fiber-based membranes, where PVC-P offered a quite tight fibrous structure compared to the PVC-R material. Contact angle studies revealed much better wetting of the PVC-P material over the PVC-R, which correlated with the adsorption studies using cationic dyes like CV and MV. Those dyes were removed from the aqueous solutions with the highest effectiveness above pH_{ZPC} values in slightly alkali media. Kinetic studies show the possibility of reusing the membrane by implementing the desorption of dyes. The results demonstrated that PVC waste can be successfully utilized in electrospinning, and the obtained fibrous membranes show great potential for the application in water treatment processes, e.g., for industrial purposes.

Acknowledgements

This work was supported by the Miniatura grant financed from the National Science Centre (NCN) under the grant number: DEC-2024/08/X/ST11/00498 and the National Science Foundation under the grant program International Research Experience for Students (NSF IRES 21072201 SOLARIS).

References

1. Lewandowski K., Skórczewska K., A brief review of poly(vinyl chloride) (PVC) recycling, *Polymers*, **14**: 3035, 2022, https://doi.org/10.3390/polym14153035.
2. Xu Z., Kolapkar S.S., Zinchik S., Bar-Ziv E., McDonald A.G., Comprehensive kinetic study of thermal degradation of polyvinylchloride (PVC), *Polymer Degradation*

and Stability, **176**: 109148, 2020, https://doi.org/10.1016/j.polymdegradstab.2020.109148.

3. Liu L., Yan B., Liu T., Zhang Y., Du R., Wang J., Chen G., Cheng Z., Chemical recycling of polyvinyl chloride: Recent progress in pretreatment dechlorination and chlorine recycling, *Resources, Conservation and Recycling*, **222**: 108471, 2025, https://doi.org/10.1016/j.resconrec.2025.108471.
4. Wagner S., Schlummer M., Application of solvent-based dissolution for the recycling of polyvinylchloride flooring waste containing restricted phthalate plasticizers, *Resources, Conservation and Recycling*, **211**: 107889, 2024, https://doi.org/10.1016/j.resconrec.2024.107889.
5. Skórczewska K., Szulc J., Lewandowski K., Ligocka A., Wilczewski S., Modification of poly(vinyl chloride) with bio-based cassia oil to improve thermo-mechanical and antimicrobial properties, *Materials*, **16**: 2698, 2023, https://doi.org/10.3390/ma16072698.
6. Youness F., Akhtiyar S., Tehrani-Bagha A., Bilbeisi R.A., Progress in modified electrospun PVC membranes: Toward sustainable solutions for environmental remediation, *Separation and Purification Technology*, **359**: 130456, 2025, https://doi.org/10.1016/j.seppur.2024.130456.
7. Bonakdar M.A., Rodrigue D., Electrospinning: Processes, structures, and materials, *Macromol*, **4**(1): 58–103, 2024, https://doi.org/10.3390/macromol4010004.
8. Stramarkou M., Tzegiannakis I., Christoforidi E., Krokida M., Use of electrospinning for sustainable production of nanofibers: A comparative assessment of smart textiles-related applications, *Polymers*, **16**(4): 514, 2024, https://doi.org/10.3390/polym16040514.
9. Escriba Flores A.A., Sanches de Almeida D., Lopes Aguiar M., Cava C.E., Enhanced air filtration efficiency through electrospun PVC/PVP/MWCNTs nanofibers: Design, optimization, and performance evaluation, *ACS Omega*, **9**(36): 37771–37779, 2024, https://doi.org/10.1021/acsomega.4c03628.
10. Zulfi A., Hartati S., Nur'aini S., Noviyanto A., Nasir M., Electrospun nanofibers from waste polyvinyl chloride loaded silver and titanium dioxide for water treatment applications, *ACS Omega*, **8**(26): 23622–23632, 2023, https://doi.org/10.1021/acsomega.3c01632.
11. Wang Z., Kang S.B., Yang E., Won S.W., Preparation of adsorptive polyethyleneimine/polyvinyl chloride electrospun nanofiber membrane: Characterization and application, *Journal of Environmental Management*, **316**: 115155, 2022, https://doi.org/10.1016/j.jenvman.2022.115155.
12. Amalia R., Noviyanto A., Rahma L.A., Merita, Labanni A., Fahroji M., Purwajanti S., Hapidin D.A., Zulfi A., PVC waste-derived nanofiber: Simple fabrication with high potential performance for PM removal in air filtration, *Sustainable Materials and Technologies*, **40**: e00928, 2024, https://doi.org/10.1016/j.susmat.2024.e00928.

13. Mani S., Bharagava R.N., Exposure to Crystal Violet, Its Toxic, Genotoxic and carcinogenic effects on environment and its degradation and detoxification for environmental safety, in: de Voogt W. (ed.), *Reviews of Environmental Contamination and Toxicology*, Vol. 237, pp. 71–104, Springer, Cham, 2016, https://doi.org/10.1007/978-3-319-23573-8_4.

14. Kua T.L., Kooh M.R.R., Dahri M.K., Zaidi N.A.H.M., Lu Y.C., Lim L.B.L., Aquatic plant, Ipomoea aquatica, as a potential low-cost adsorbent for the effective removal of toxic methyl violet 2B dye, *Applied Water Science*, **10**: 243, 2020, https://doi.org/10.1007/s13201-020-01326-9.

15. Chi Z., Liu R., Zhao X., Sun Y., Yang B., Gao C., Study on the genotoxic interaction of methyl violet with calf thymus DNA, *Applied Spectroscopy*, **63**(12): 1331–1335, 2009, https://doi.org/10.1366/000370209790109085.

16. Cruz P.P.R., da Silva L.C., Fiuza-Jr R.A., Polli H., Thermal dehydrochlorination of pure PVC polymer: Part I – thermal degradation kinetics by thermogravimetric analysis, *Journal of Applied Polymer Science*, **138**: e50598, 2021, https://doi.org/10.1002/app.50598.

17. Nishibata H., Uddin Md.A., Kato Y., Simultaneous degradation and dechlorination of poly (vinyl chloride) by a combination of superheated steam and CaO catalyst/adsorbent, *Polymer Degradation and Stability*, **179**: 109225, 2020, https://doi.org/10.1016/j.polymdegradstab.2020.109225.

18. Briesemeister M., Gómez-Sánchez J.A., Bertemes-Filho P., Pezzin S.H., PVC/CNT electrospun composites: Morphology and thermal and impedance behavior, *Polymers*, **16**(20): 2867, 2024, https://doi.org/10.3390/polym16202867.

19. Zhao J., Ma H., Huang H., Zhang J., Chen Y., Experimental investigation and numerical modeling of oxidative pyrolysis mechanism of mining PVC cable sheath, *Journal of Thermal Analysis and Calorimetry*, **147**: 14479–14490, 2022, https://doi.org/10.1007/s10973-022-11723-8.

20. Lu Yh., Chen Zl., Lu Yw., Synthesis, characterization and thermal behavior of plasticized poly (vinyl chloride) doped with folic acid-modified titanium dioxide, *Scientific Reports*, **12**: 3379, 2022, https://doi.org/10.1038/s41598-022-07177-5.

21. Gartili A., Caillol S., Briou B., Lapinte V., One step beyond for CNSL-based plasticizers for PVC: Use of cardol, *European Journal of Lipid Science & Technology*, **126**: e2400086, 2024, https://doi.org/10.1002/ejlt.202400086.

22. Pham Le Q., Uspenskaya M.V., Olekhnovich R.O., Baranov M.A., The mechanical properties of PVC nanofiber mats obtained by electrospinning, *Fibers*, **9**(1): 2, 2021, https://doi.org/10.3390/fib9010002.

23. Boraei S.B.A., Bakhshandeh B., Mohammadzadeh F., Haghighi D.M., Mohammadpour Z., Clay-reinforced PVC composites and nanocomposites, *Heliyon*, **10**: e29196, 2024, https://doi.org/10.1016/j.heliyon.2024.e29196.

24. Lenzi L., Esposti, M.D., Braccini S., Siracusa C., Quartinello F., Guebitz G.M., Puppi D., Morselli D, Fabbri P., Further step in the transition from conventional

plasticizers to versatile bioplasticizers obtained by the valorization of levulinic acid and glycerol, *ACS Sustainable Chemistry & Engineering*, **11(**25): 9455–9469, 2023, https://doi.org/10.1021/acssuschemeng.3c01536.

25. Quoc Pham L., Uspenskaya M.V., Olekhnovich R.O., Olvera Bernal R.A., A review on electrospun PVC nanofibers: fabrication, properties, and application, *Fibers*, **9**(2): 12, 2021, https://doi.org/10.3390/fib9020012.

26. Zhong Y., Wang K., Guo C., Kou Y., Hassan A., Lu Y., Wang J., Wang W., Competition adsorption of malachite green and rhodamine B on polyethylene and polyvinyl chloride microplastics in aqueous environment, *Water Science & Technology*, **86**(5): 894–908, 2022, https://doi.org/10.2166/wst.2022.252.

27. Jang M.H., Kim M.S., Han M., Kwak D.H., Experimental application of a zero-point charge based on pH as a simple indicator of microplastic particle aggregation, *Chemosphere*, **299**: 134388, 2022, https://doi.org/10.1016/j.chemosphere.2022.134388.

28. Pietrzyk P., Borowska E.I., Hejduk P., Camargo B.C., Warczak M., Nguyen P.T., Pregowska A., Gniadek M., Szczytko J., Wilczewski S., Osial M., Green composites based on volcanic red algae *Cyanidiales,* cellulose, and coffee waste biomass modified with magnetic nanoparticles for the removal of methylene blue, *Environmental Science and Pollution Research*, **30**: 62689–62703, 2023, https://doi.org/10.1007/s11356-023-26425-3.

29. Smith B.C., The infrared spectra of polymers III: Hydrocarbon polymers, *Spectroscopy*, **36**(11): 22–25, 2021, https://doi.org/10.56530/spectroscopy.mh7872q7.

30. Zhao J, Liu H., Xue P., Tian S., Sun S., Highly-efficient PVDF adsorptive membrane filtration based on chitosan@CNTs-COOH simultaneous removal of anionic and cationic dyes, *Carbohydrate Polymers*, **274**(15): 118664, 2021, https://doi.org/10.1016/j.carbpol.2021.118664.

31. Sultana S., Chakraborty D., Parvez D.A., Chandan M.R., Rahaman M., Polymeric membranes for advanced separation and sensing: Materials and mechanisms for emerging applications – A review, *Chemistry an Asian Journal*, **28**(18): e00714, 2025, https://doi.org/10.1002/asia.202500714.

32. Elnagar E.R., Hamdy G., Abdallah H., Ali S.S., Taher F.A., Enhanced performance of polyvinylidene fluoride with triethanolamine and polyethylene glycol ultrafiltration membrane for textile wastewater treatment, *International Journal of Environmental Science and Technology*, **22**: 5529–5542, 2025, https://doi.org/10.1007/s13762-024-05938-5.

33. Rianjanu A., Recent advances in electrospun nanofiber membranes for dye filtration: A focused mini-review, *Environmental Chemistry and Safety*, **1**(2): 9600018, https://doi.org/10.26599/ECS.2025.9600018.

34. Khan I.A., Khan A.U., Butt M.S., Janjua A., Uddin E., Deen K.M., Sadiq R., Ahmad N.M., Dye removal from contaminated water through PES membranes enhanced with the incorporation of switchable polyacrylic acid grafted on graphene

oxide, *ACS Omega*, **10**(26): 28178–28190, 2025, https://doi.org/10.1021/acsomega.5c02815.

35. Agaguena A., Benbellat N., Khaoua O., Bendaikha T., Kinetic adsorption of methyl blue dye from aqueous solution by PVC/PVC-based copolymer containing quaternary amine, *Analytical Science*, **39**: 1371–1383, 2023, https://doi.org/10.1007/s44211-023-00356-y.

36. Landarani M., Arab Chamjangali M., Bahramian B., Preparation and characterization of a novel chemically modified PVC adsorbent for methyl orange removal: Optimization, and study of isotherm, kinetics, and thermodynamics of adsorption process, *Water, Air & Soil Pollution*, **231**: 513, 2020, https://doi.org/10.1007/s11270-020-04874-7.